Technical Report No. 32-354

A New Horn Antenna with Suppressed Sidelobes and Equal Beamwidths

P. D. Potter

JET PROPULSION LABORATORY
CALIFORNIA INSTITUTE OF TECHNOLOGY
PASADENA, CALIFORNIA

February 25, 1963

Technical Report No. 32-354

A New Horn Antenna with Suppressed Sidelobes and Equal Beamwidths

P. D. Potter

R Stevens

Robertson Stevens, *Chief*
Communications Elements Research Section

JET PROPULSION LABORATORY
CALIFORNIA INSTITUTE OF TECHNOLOGY
PASADENA, CALIFORNIA

February 25, 1963

Prepared Under Contract No. NAS 7-100
National Aeronautics & Space Administration

CONTENTS

FIGURES

ACKNOWLEDGMENT

The author is grateful to Mr. Frank McCrea, who fabricated many of the horn components and performed all of the experimental tests, and to Mr. Arthur Ludwig, who suggested the three-dimensional representation for the TE_{11}° and TM_{11}° mode radiation patterns.

ABSTRACT

For many years pyramidal and conical horns have been used at UHF and microwave frequencies for applications requiring a simple type of antenna with medium gain. In this Report a technique is presented for excitation of horns which simultaneously results in complete beamwidth equalization in all planes, complete phase center coincidence, and at least 30-db sidelobe suppression in the electric plane. An analysis of the theory of this technique is presented, together with complete experimental data.

I. INTRODUCTION AND PREVIOUS WORK

For many years pyramidal horns have been used at UHF and microwave frequencies for applications requiring a simple type of antenna with medium gain (i.e., 10-30 db above isotropic) and are popular as antenna range illuminators, gain standards, and reflector illuminators.

Most of the large bulk of work done on pyramidal horns has been concerned with those of rectangular cross-section (Ref. 1-4), partly for historical reasons and also because of the attendant simple transition to standard rectangular waveguide. This work has been primarily concerned with the dominant $TE_{01}^{\square}$ or $TE_{10}^{\square}$ modes, although some effort has been applied to high-order rectangular modes (Ref. 1), notably for monopulse and beamshaping applications.

A relatively recent development, the diagonal-horn antenna (Ref. 5 and 6), appears to have somewhat superior sidelobe and beamwidth performance to the standard pyramidal horn. The aperture distribution in this horn, an in-phase superposition of the TE_{10} and TE_{01} modes, bears a strong physical resemblance to the aperture distribution in a conical horn, i.e., a pyramidal horn of circular cross-section.

It is well-known that the conical horn, operating in the dominant TE_{11}° mode, has effectively a tapered aperture distribution in the electric plane. For this reason its beamwidths in the electric and magnetic planes are more nearly equal than those with a square pyramidal horn—a valuable feature for polarization diversity applications. An additional result of this tapered electric-plane distribution is a more favorable sidelobe structure than with the square horn. The conical horn has received a reasonable amount of attention in the literature (see pp. 336-341 of Ref. 1 and Ref. 7-10), although it is not often used in practice because of its relative incompatibility with rectangular waveguide.

One of the important characteristics of horn radiators for most applications is the sidelobe level. It is important in antenna range, anechoic chamber, and standard gain applications because of multipath considerations. In reflector illuminator applications, it is important because of main-beam efficiency and spurious wide-angle radiation effects. For the latter application, electric- and magnetic-plane phase center coincidence is also of importance. For many applications, equality of principal-plane beamwidths is an important third consideration.

In this Report, a technique is presented (Ref. 11) which simultaneously results in complete beamwidth equalization in all planes, complete phase center coincidence, and at least 30-db sidelobe suppression in the electric plane. The magnetic-plane performance is unaffected. The technique, referred to as the "dual-mode conical horn," utilizes a conical horn excited at the throat region in both the dominant TE_{11}° mode and the higher-order TM_{11}° mode. These two modes are then excited in the horn aperture with the appropriate relative amplitude and phase to effect sidelobe suppression and beamwidth equalization. Phase center coincidence follows as a result. The predicted radiation pattern characteristics are easily derived, as is the technique for mode generation and control. Several experimental configurations were tested and were shown to have the predicted characteristics.

Although not yet investigated in detail, it should be pointed out that the same technique can be extended to use in horns of rectangular cross section.[a] Another recent discovery, also not yet investigated in detail, is that use of the TE_{12}° mode in addition to the TE_{11}° and TM_{11}° modes can provide H-plane sidelobe suppression in addition to the normal dual mode horn characteristics. In general, it is felt that the horn described in this report is only the first step in the technique of utilizing orthogonal waveguide modes to produce practical horn antennas with new radiation characteristics.

[a]Private communication from Mr. P. A. Jensen.

II. RADIATION CHARACTERISTICS OF THE DUAL-MODE CONICAL HORN

Some effort has been expended toward use of the higher-order modes in pyramidal and sectorial horns to effect more desirable electric-plane radiation characteristics. Success has been only fair, however, since in general the associated radiation function argument varies with mode order. Certain pairs of these modes, however, have radiation functions with the same argument, the only major difference being an additional envelope factor in one of the modes, varying rapidly in the main beam region and remaining relatively constant at larger angles. It is thus possible, by using this approach, to effect almost complete cancellation of radiation in all directions, except those within the main beam.

The radiation characteristics of the dominant TE_{11}° mode and the TM_{11}° mode in conical horns are worthy of detailed consideration. Based on work by Chu (Ref. 12), Silver (Ref. 1) developed the radiation functions for open-end circular cross-section pipe, assumed to be equivalent to a conical horn. In this analysis the boundary problems arising due to the aperture discontinuity are neglected (Schorr and Beck make the same approximation in their conical analysis in Ref. 8). Obviously, the boundary condition inside conical waveguide cannot be satisfied by cylindrical TE° modes, but must also utilize the cylindrical TM° modes. This problem, not peculiar to conical horns, becomes progressively more severe with increasing horn flare angle. The effect is qualitatively described (Ref. 4) as "aperture phase error," although this concept is incompatible with the cylindrical TE modes. (It is not, however, incompatible with the spherical TE modes used by Schorr and Beck.) It is reasonable to assume that all noncompensated conical horns radiate in both the TE_{11}° and TM_{11}° modes. It has previously been erroneously assumed that presence of the TM_{11}° mode is always deleterious to the horn performance. The error in this assumption can easily be shown.

The polar and azimuthal component radiation patterns of the TE_{11}° mode, respectively, are given by Silver (Ref. 1) as follows:[b]

$$E_{\theta H} = -\frac{\omega\mu}{2R}\left(1 + \frac{\beta_{11H}\cos\theta}{k}\right) J_1(K_{11H}a) \left[\frac{J_1(ka\sin\theta)}{\sin\theta}\right] \sin\phi e^{-jkR} \qquad (1)$$

and

$$E_{\phi H} = -\frac{ka\omega\mu}{2R}\left(\frac{\beta_{11H}}{k} + \cos\theta\right) J_1(K_{11H}a) \left[\frac{J_1'(ka\sin\theta)}{1 - \left(\frac{k\sin\theta}{K_{11H}}\right)^2}\right] \cos\phi e^{-jkR} \qquad (2)$$

where

ω = radian frequency

μ = permeability

k = free-space propagation constant

a = aperture half diameter

J_1 = first-order Bessel function of the first kind

J_1' = first derivative of J_1 with respect to its argument

$K_{11H}a$ = first root of $J_1' = 1.841$

θ = polar angle

ϕ = azimuth angle

R = distance from the aperture center to the observation point

$j = \sqrt{-1}$

$\beta_{11H} = \sqrt{k^2 - K_{11H}^2}$

The coordinate system, as well as the aperture electric-field distribution, is shown in Fig. 1. In Fig. 2 the E- and H-plane calculated and measured patterns are shown for a particular example. As expected, Fig. 2a indicates the presence of spurious TM_{11}° energy. This energy cannot affect Fig. 2b, however, since TM_{11}° modes have no azimuthal electric field component in any direction (Ref. 1).

The polar radiation pattern for the TM_{11}° mode is given by Silver (Ref. 1) as follows:

$$E_{\theta E} = -\left(\frac{kaK_{11E}}{2R}\right)\left(\frac{\beta_{11E}}{k} + \cos\theta\right)\left[\frac{J_1'(K_{11E}a)}{1 - \left(\frac{K_{11E}}{k\sin\theta}\right)^2}\right] \left[\frac{J_1(ka\sin\theta)}{\sin\theta}\right] \sin\phi e^{-jkR} \qquad (3)$$

$$E_{\phi E} = 0$$

where

$K_{11E}a$ = first root of $J_1 = 3.832$

$\beta_{11E} = \sqrt{k^2 - K_{11E}^2}$

[b]The aperture is assumed perfectly matched to space here.

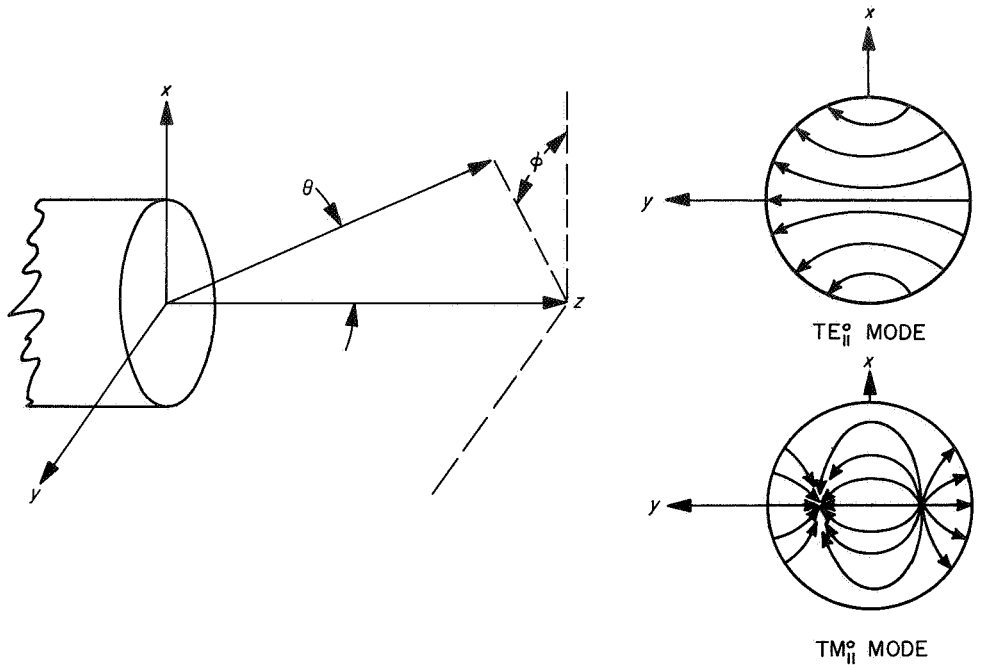

Fig. 1. Radiation coordinate system

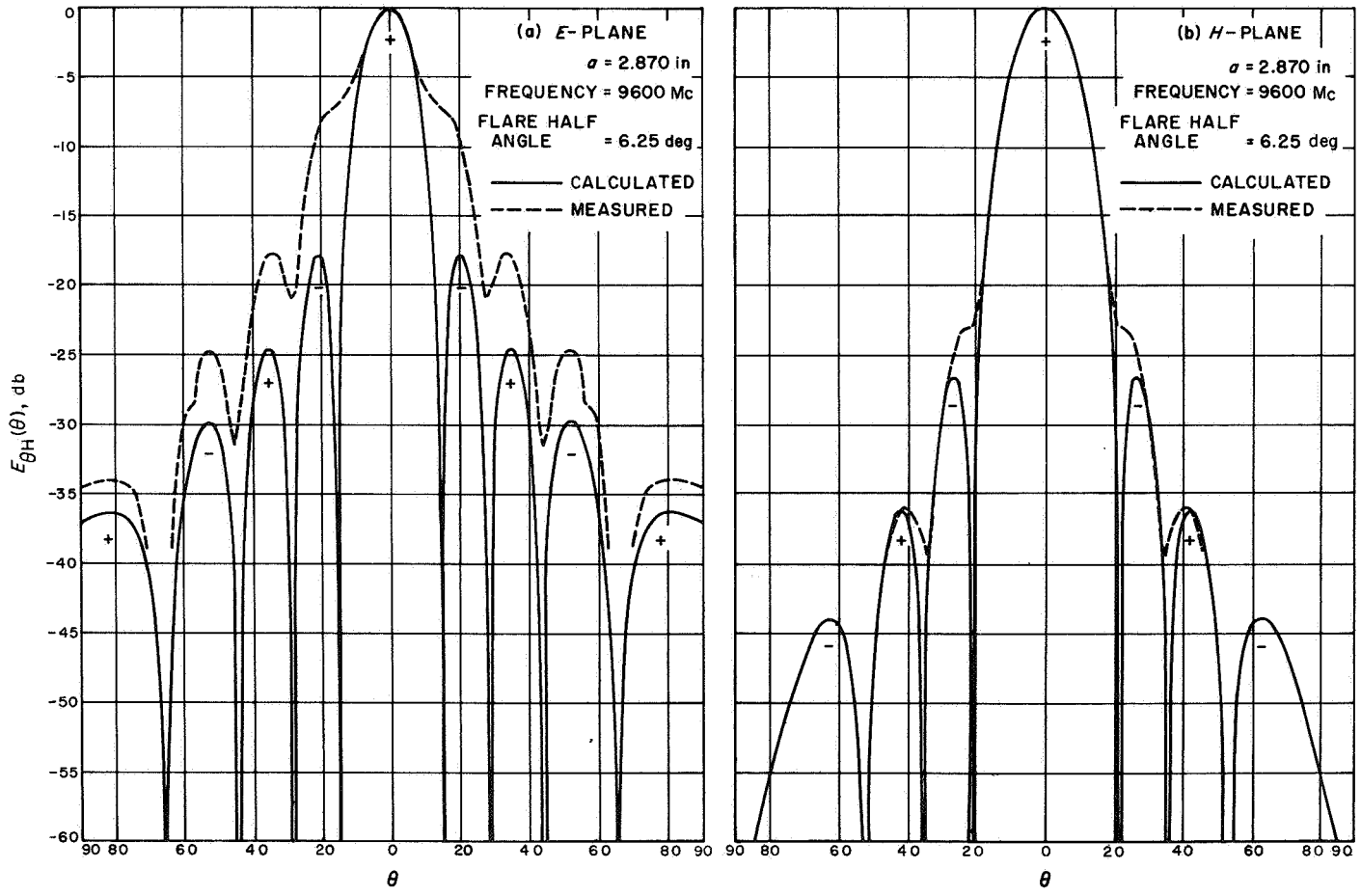

Fig. 2. Radiation patterns for the TE_{11}^{o} mode

The aperture electric-field distribution is shown in Fig. 1. The calculated TM_{11}° radiation pattern in the plane of maximum radiation for the horn configuration used in Fig. 2 is shown in Fig. 3.

A striking similarity in the E-plane TE_{11}° and TM_{11}° sidelobe structure is evident in Fig. 2 and 3. This feature is also evident from a comparison of Eq. (1) and (3). By eliminating constants and assuming that cos θ is unity,

$$E_{\theta H} \approx \sin\phi\left[\frac{J_1(u)}{u}\right] \tag{4}$$

and

$$E_{\theta E} \approx \left[\frac{1}{1-\left(\frac{K_{11E}a}{u}\right)^2}\right]\sin\phi\left[\frac{J_1(u)}{u}\right] \tag{5}$$

where

$$u = ka\sin\theta \tag{6}$$

For large u, the bracketed factor in (5) becomes very nearly unity, allowing the possibility of sidelobe cancellation. This factor becomes infinite and changes sign at the first zero of the $J_1(u)$ function. If, therefore, Eq. (4) and (5) are subtracted, partial cancellation occurs beyond the first root with electric-plane beam broadening in the main beam. The radiation characteristics of the TE_{11}° and TM_{11}° modes are more clearly seen in Fig. 4, which are three-dimensional representations similar to those used by Jahnke and Emde (Ref. 13).

In order to predict the performance of the dual-mode conical horn in the electric plane, Eq. (1) and (3) may be simplified and combined as follows:

$$E_{\theta T} = \left[\left(1+\frac{\beta_{11H}}{k}\cos\theta\right) - \alpha\frac{\left(\frac{\beta_{11E}}{k}\right)+\cos\theta}{1-\left(\frac{K_{11E}}{k\sin\theta}\right)^2}\right]\left[\frac{J_1(ka\sin\theta)}{\sin\theta}\right] \tag{7}$$

or, in approximate form,

$$E_{\theta T} \approx \left[1-\frac{\alpha}{1-\left(\frac{K_{11E}a}{u}\right)^2}\right]\left[\frac{J_1(u)}{u}\right] \tag{8}$$

where α = arbitrary constant defining the relative power in the TE_{11}° and TM_{11}° modes.

Equation (8) is plotted in Fig. 5 for various values of α including $\alpha = 0$, which corresponds to the dominant single-mode case. Although a range of α in the region of $\alpha = 0.6$ is most interesting, particular applications will dictate the exact value chosen; for example, a value of $\alpha = 0.653$ will equalize the E- and H-plane half-power beamwidths and make the phase centers coincident. This condition also results in the minimum possible backlobe.[c]

Measured data for the dual-mode conical horn are shown in Fig. 6 for the E-, 45-deg, and H-planes. The calculated E-plane data utilized Eq. (7). The 45-deg plane pattern is defined as the polarization component parallel to the $\phi = \pi/2$ plane, but measured in either the $\phi = \pi/4$ or $3\pi/4$ planes. Because of its redundancy, the 45-deg plane is more important than the E- or H-plane for many applications (Ref. 14). Two other aperture sizes were also tested in the dual-mode configuration; the associated E-plane radiation patterns are shown in Fig. 7 and 8.

One other horn characteristic, the phase pattern, is of concern in reflector illumination applications (Ref. 14). The serrodyne (Ref. 15) test setup used to measure this horn property is shown schematically in Fig. 9. The measured E-plane phase pattern and phase center position is shown in Fig. 10 for the dual-mode horn with $a = 2.870$ in. Other planes are virtually identical.

A simple over-all measure of horn performance is the beam efficiency, i.e., the fractional radiated power between $\theta = 0$ and $\theta = \theta_1$, as a function of θ_1. Figure 11 shows this factor in the E-, 45-deg, and H-planes for dual-mode conical, square, single-mode conical, and diagonal horn configurations. The latter is calculated from data published by Love (Ref. 5). All curves are normalized to the same half-power beamwidth and all include cross-polarized energy. It can be seen that the popular diagonal horn would be a good competitor to the dual-mode conical horn if it were not for the 45- and 135-deg planes (unfortunately, the most important planes). It can also be seen that the dual mode conical horn is good in the H-plane, even though no sidelobe suppression is effected in that plane.

[c]Private communication from Mr. J. Ajioka.

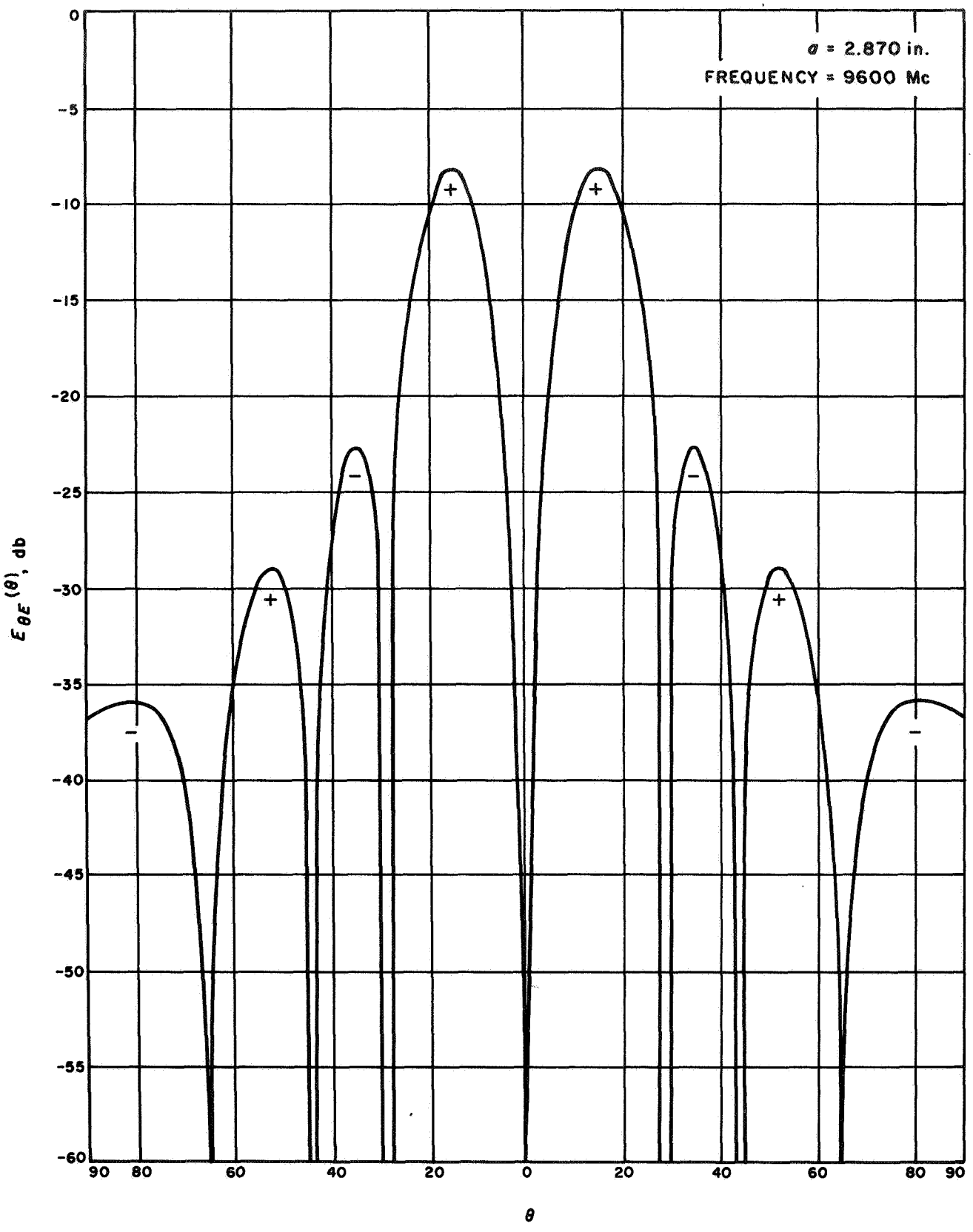

Fig. 3. *E*-plane pattern for TM_{11}^{o} mode

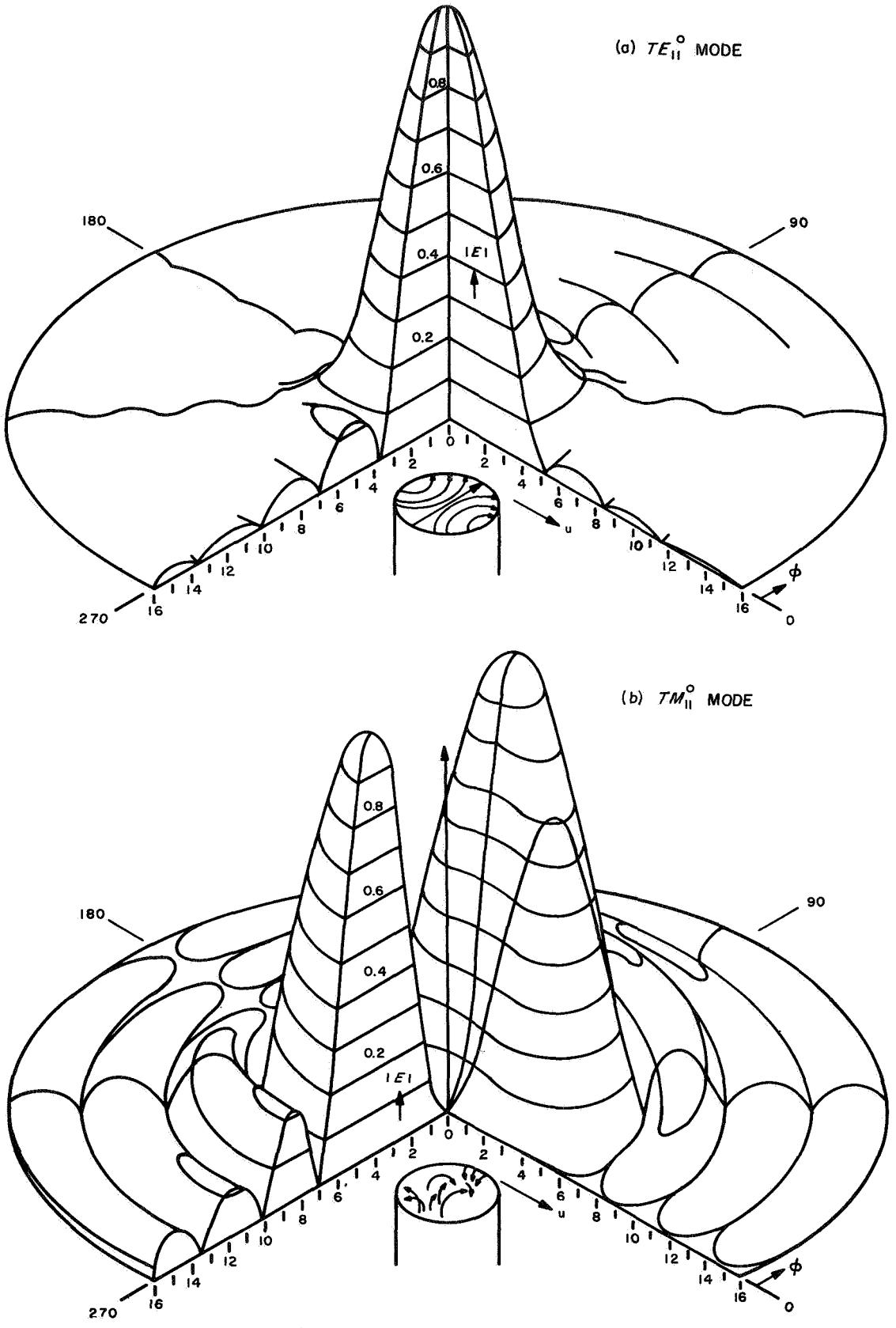

Fig. 4. Three-dimensional radiation patterns

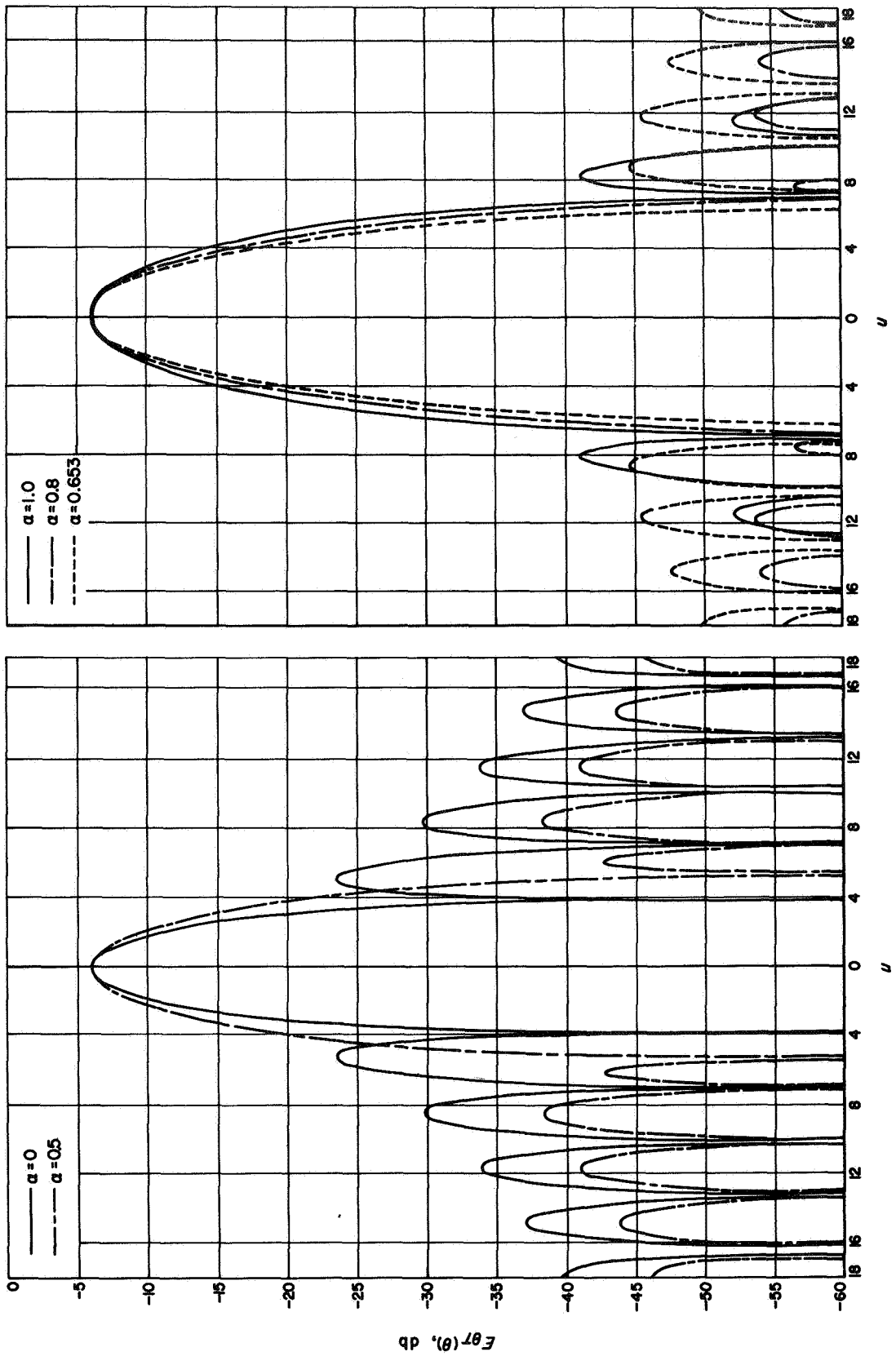

Fig. 5. Calculated dual-mode conical-horn patterns

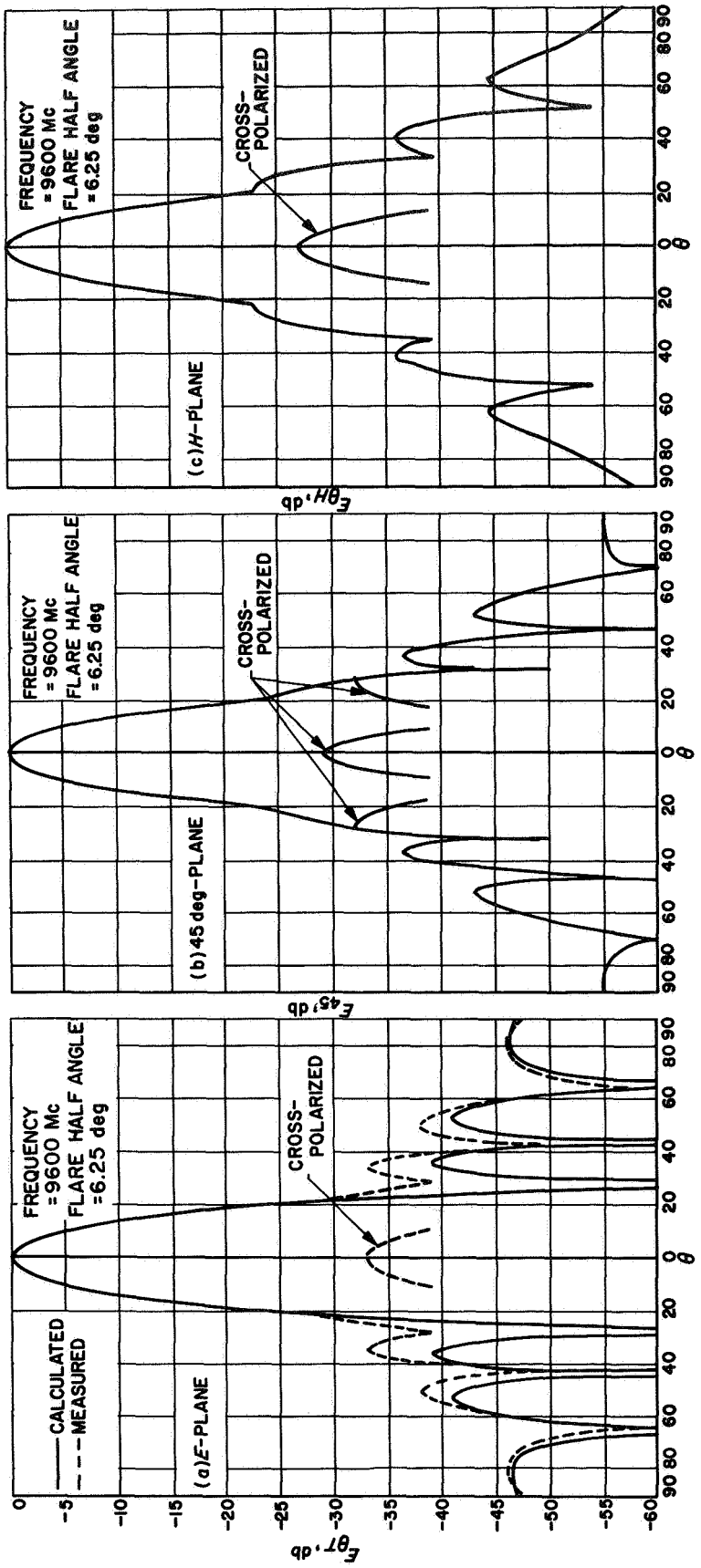

Fig. 6. Dual-mode patterns for $a = 2.870$ in.

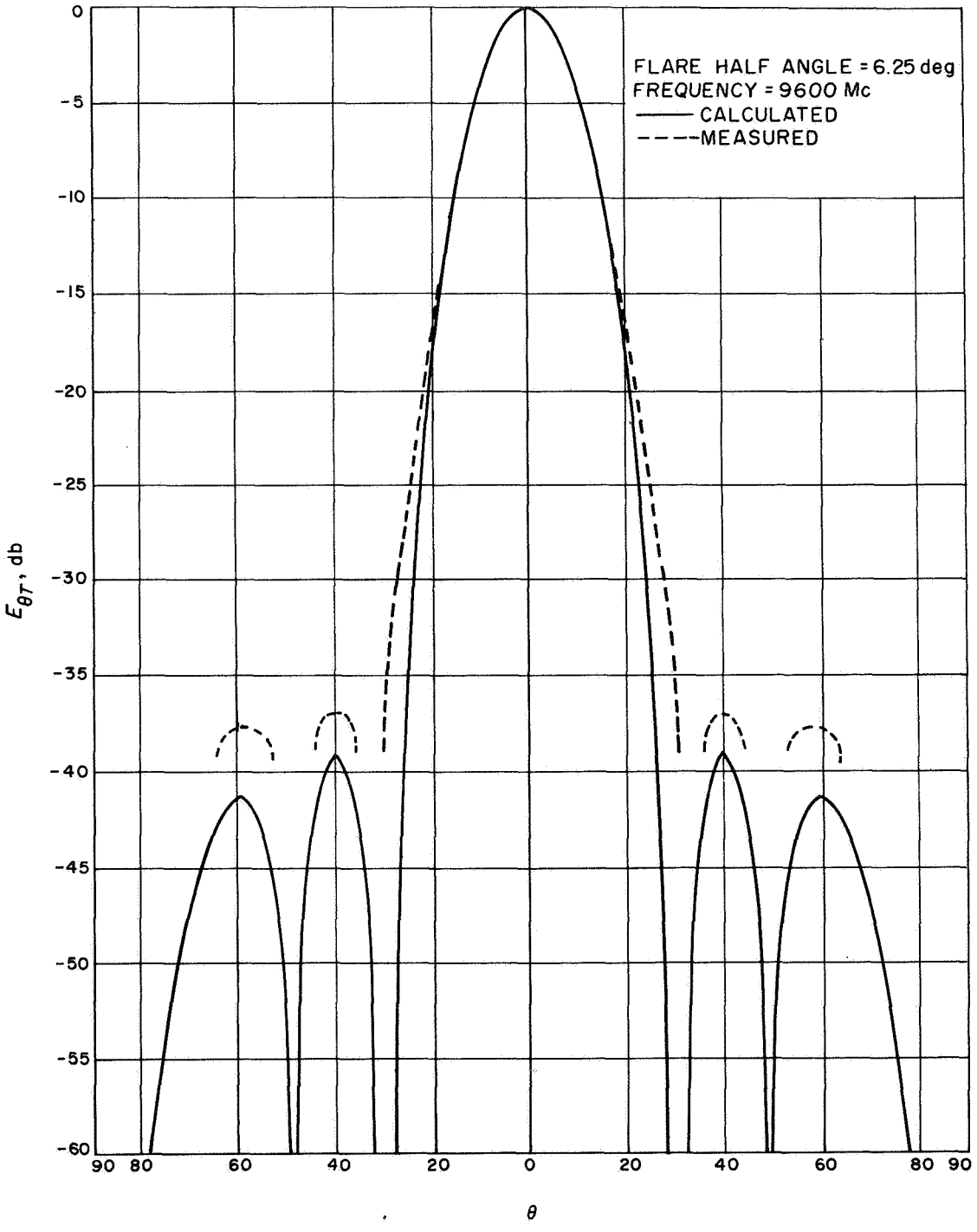

Fig. 7. *E*-plane dual-mode pattern for $a = 2.635$ in.

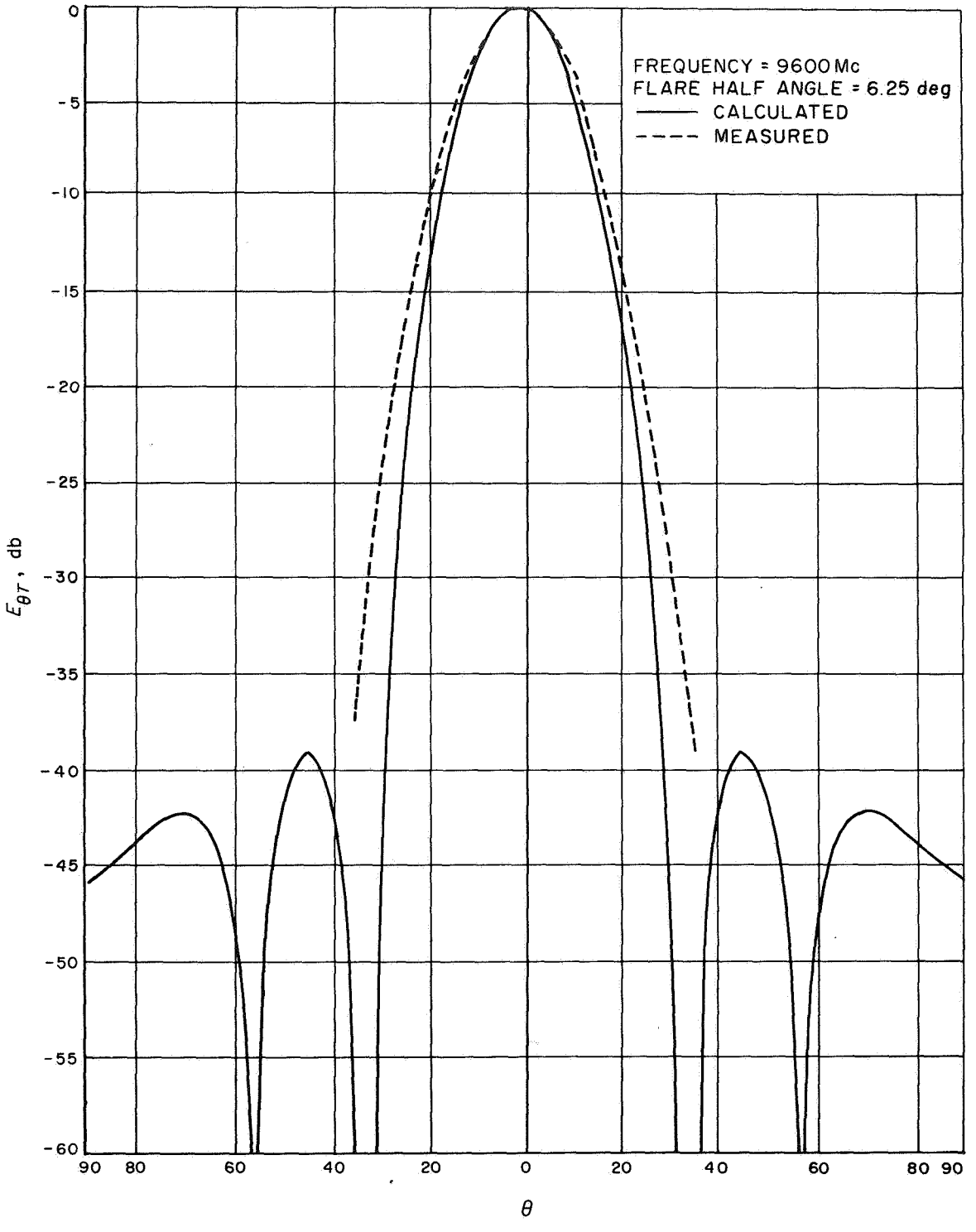

Fig. 8. *E*-plane dual-mode pattern for $a = 2.400$ in.

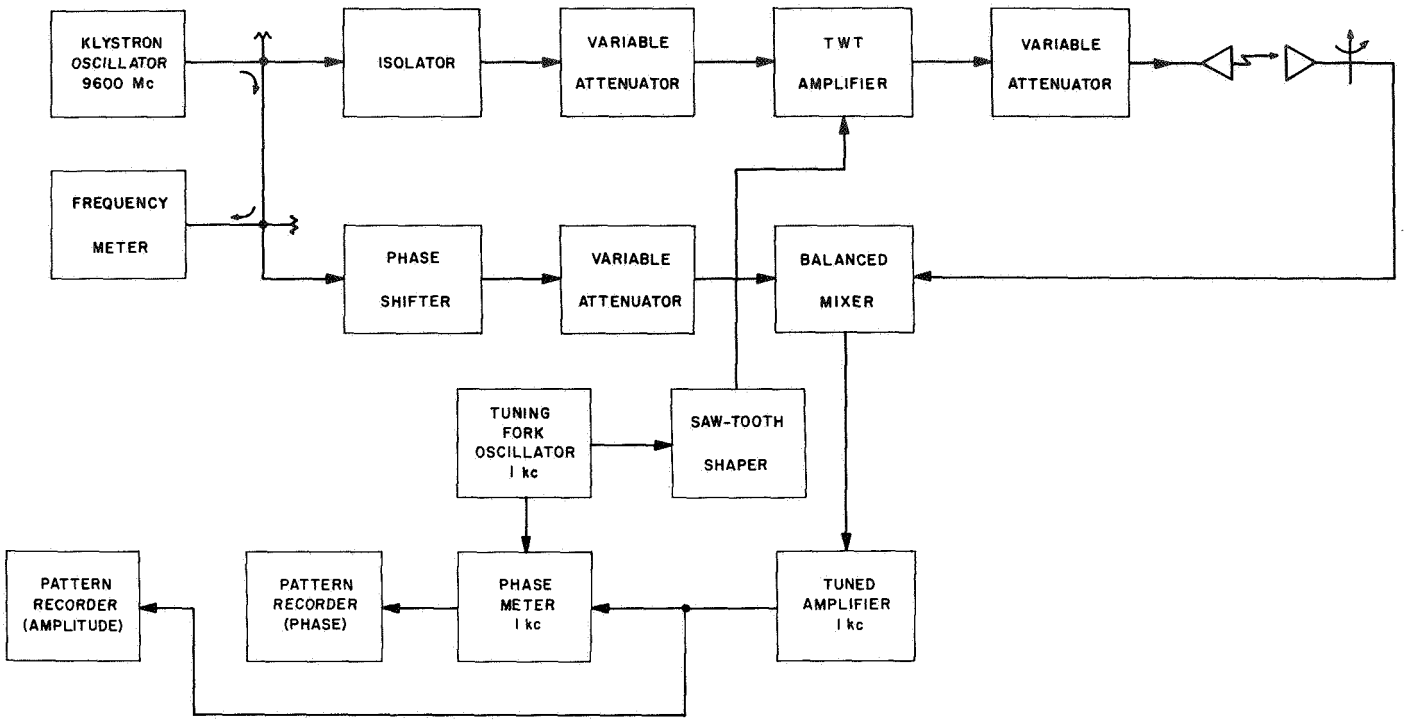

Fig. 9. Serrodyne phase measurement setup

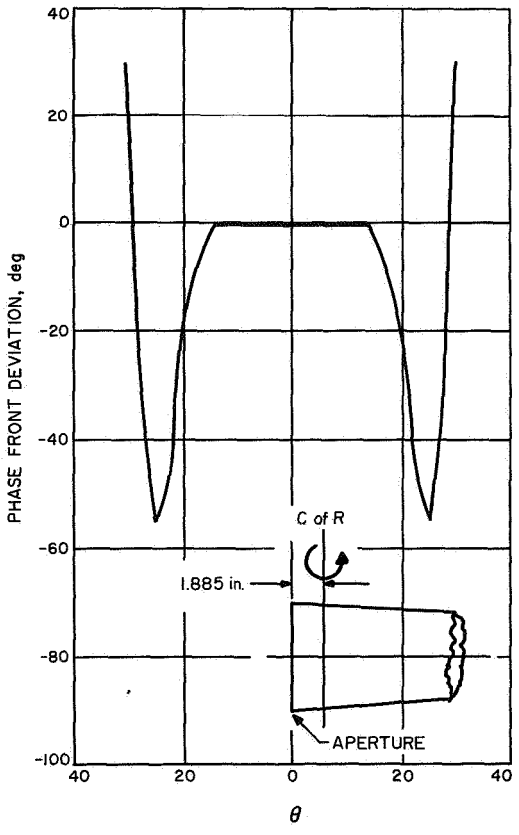

Fig. 10. Measured dual-mode conical-horn phase center characteristics

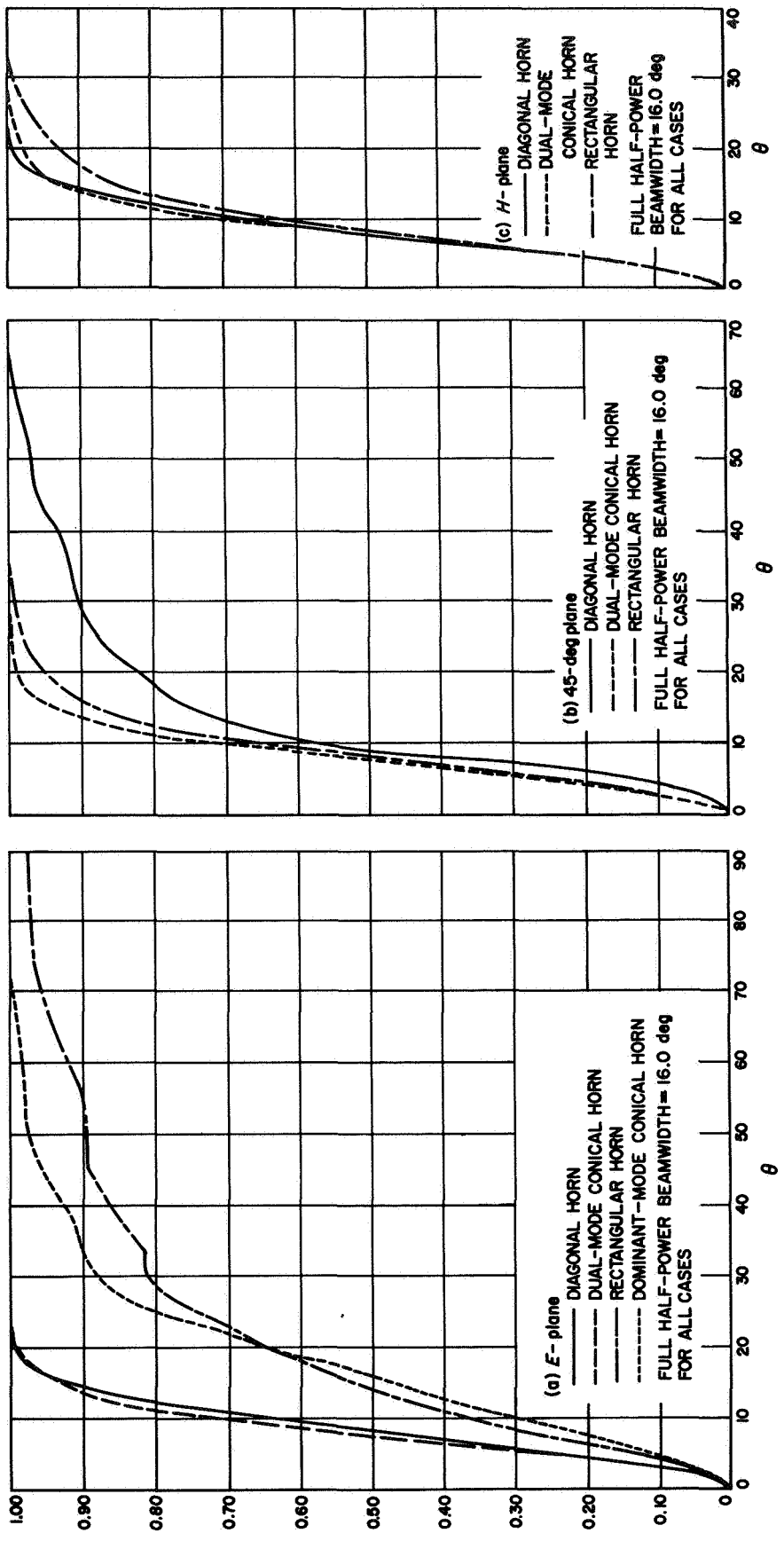

Fig. 11. Beam efficiency of various horns

III. MODE GENERATION AND CONTROL

The technique of TM_{11}° mode generation is shown qualitatively in Fig. 12, together with empirically determined parameters for the experimental horns. As can be seen in Fig. 1, the step discontinuity boundary condition of zero tangential electric field on the step surface will be largely satisfied by the TE_{11}° and TM_{11}° modes. The two diameters are chosen to satisfy the following four conditions:

1. Only TE_{11}° (and possibly TM_{01}° and TE_{21}°) can propagate to the left of the step.
2. Only TE_{11}°, TM_{01}°, TE_{21}°, TE_{01}° and TM_{11}° can propagate to the right of the step.
3. TM_{11}° is generated in the correct power ratio relative to TE_{11}°.
4. TE_{11}° and TM_{11}° have significantly different phase velocities in the phase section to the right of the step.

The unwanted TM_{01}°, TE_{21}°, and TE_{01}° modes are not excited because of symmetry in the mode generator and horn. In practice it was found that concentricity and circularity of the mode generator and horn components on the order of a few thousandths of a wavelength are necessary to make the effect of spurious modes negligible. This might pose a practical fabrication problem in the millimeter region, but is not otherwise serious.

The radial components of the assumed aperture field distributions for the TE_{11}° and TM_{11}° modes, respectively, are given by Silver (see pp. 200–234 of Ref. 1) as

$$E_{rH} = j\omega\mu \frac{J_1(K_{11H}r)}{r} \sin\phi \tag{9}$$

$$E_{rE} = j\beta_{11E} K_{11E} J_1'(K_{11E}r) \sin\phi \tag{10}$$

From a careful comparison of Eq. (1), (3), (7), (9), and (10), it can be seen that the TE_{11}° and TM_{11}° modes must have their central fields in phase in the aperture to produce the desired radiation pattern. Thus, the length of the phasing section shown in Fig. 12 must be chosen to account for the relative phase lengths of the horn for the two modes, and also for the phase of mode generation. The latter has not yet been subjected to detailed analysis, but is empirically established by the experimental data in Fig. 12.

The differential phase length of the horn flare for the TE_{11}° and TM_{11}° modes can be easily calculated by

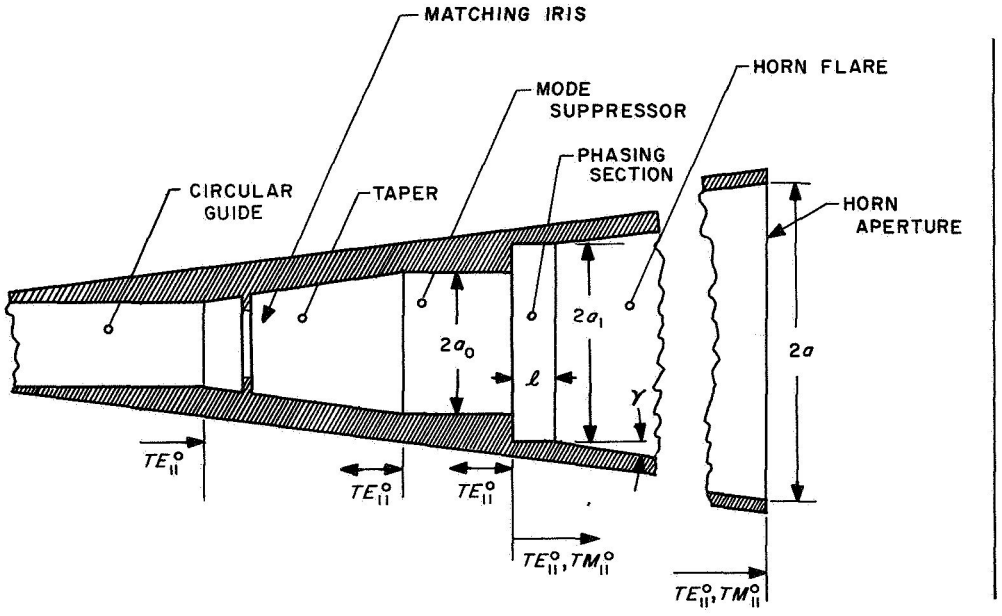

EXPERIMENTAL DATA

HORN	$2a$ in	$2a_1$ in	$2a_0$ in	ℓ in
1	5.74	1.60	1.25	0.25
2	5.27	1.60	1.25	0.40
3	4.80	1.60	1.25	0.54

γ = 6.25 deg
FREQUENCY = 9600 Mc

Fig. 12. Dual-mode conical-horn configuration

straightforward integration of the standard formula (see pp. 200-234 of Ref. 1) for waveguide phase velocity. The result is

$$\Delta\Phi_H = \cot\gamma \left\{ \left[\left(\frac{a^2}{\lambda^2} - \frac{C_H^2}{4\pi^2} \right)^{\frac{1}{2}} - \left(\frac{a^2}{\lambda^2} - \frac{C_E^2}{4\pi^2} \right)^{\frac{1}{2}} - \left(\frac{C_H}{2\pi} \cos^{-1} \frac{C_H\lambda}{2\pi a} \right) + \left(\frac{C_E}{2\pi} \cos^{-1} \frac{C_E\lambda}{2\pi a} \right) \right] \right. \quad (11)$$

$$\left. - \left[\left(\frac{a_1^2}{\lambda^2} - \frac{C_H^2}{4\pi^2} \right)^{\frac{1}{2}} - \left(\frac{a_1^2}{\lambda^2} - \frac{C_E^2}{4\pi^2} \right)^{\frac{1}{2}} - \left(\frac{C_H}{2\pi} \cos^{-1} \frac{C_H\lambda}{2\pi a_1} \right) + \left(\frac{C_E}{2\pi} \cos^{-1} \frac{C_E\lambda}{2\pi a_1} \right) \right] \right\}$$

where

$\Delta\Phi_H$ = differential phase in wavelengths

γ = horn-flare half angle

C_E = first root of $J_1 = 3.832$

C_H = first root of $J_1' = 1.841$

λ = wavelength of operation

a_1 = horn-throat half diameter

Equation (11) is plotted in Fig. 13a as a function of aperture size for various throat sizes.

The differential phase length of the phasing section in wavelengths per wavelength is given by

$$\Delta\Phi_c = \frac{\lambda}{a_1} \left[\left(\frac{a_1^2}{\lambda^2} - \frac{C_H^2}{4\pi^2} \right)^{\frac{1}{2}} - \left(\frac{a_1^2}{\lambda^2} - \frac{C_E^2}{4\pi^2} \right)^{\frac{1}{2}} \right] \quad (12)$$

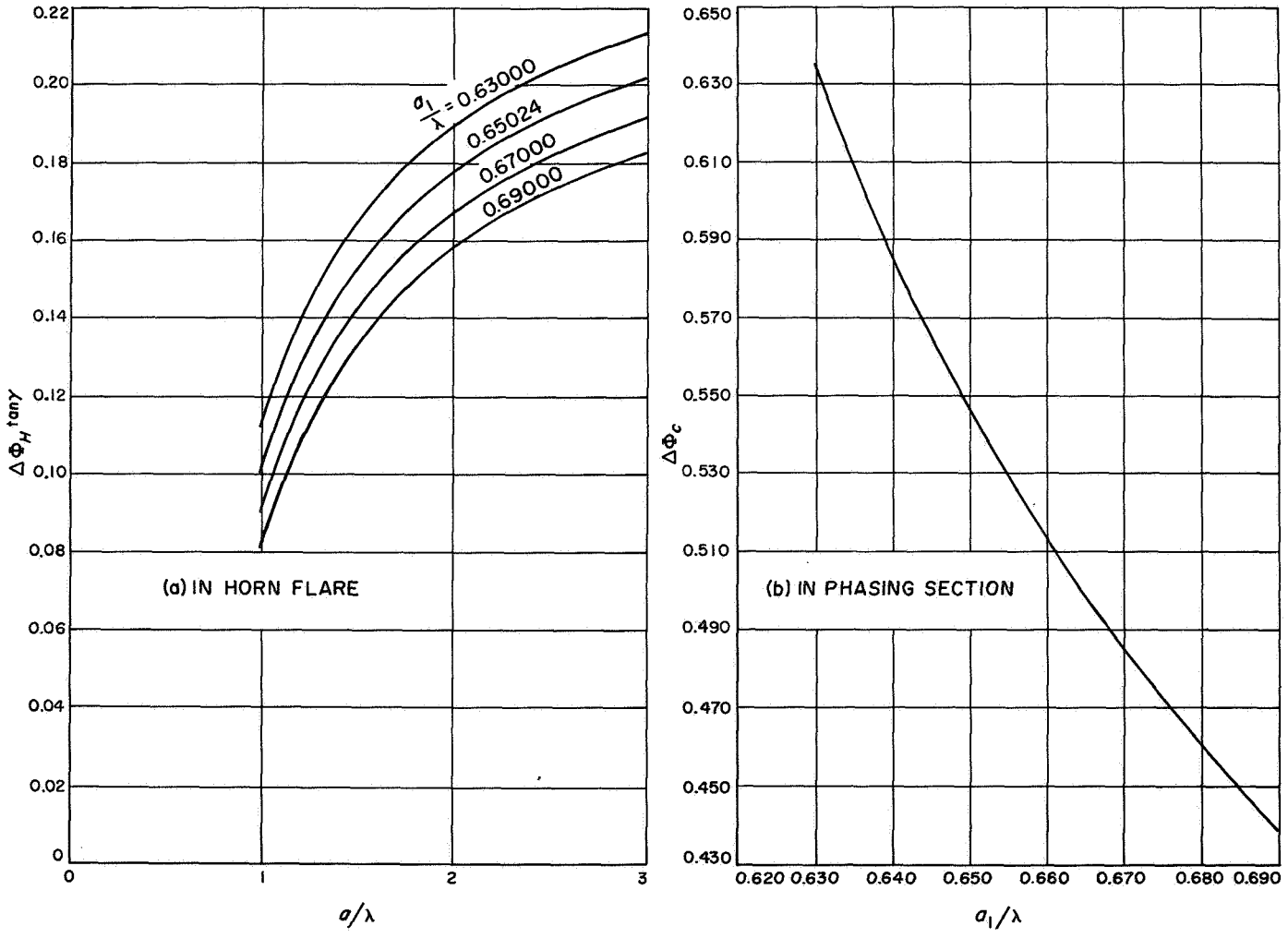

Fig. 13. Differential phase lengths

Equation (12) is plotted in Fig. 13b for the interesting range of a_1/λ. In the experimental work reported here, the phasing section length was determined empirically for the configuration $a = 2.870$ in.; Eq. (11) and (12) were then used to calculate the phasing section length change necessary for the 2.635- and 2.400-in. aperture configurations. The result, shown in Fig. 7 and 8, indicates correct performance. The design procedure is thus adequately established with the use of Fig. 5, 12, and 13.

One final point in the design should be considered—impedance matching. The VSWR of the unmatched horn for the configuration in Fig. 12 was found to be 1.2:1, a value predicted by the TE_{11}°-mode wave impedance change at the step discontinuity. Data given in Marcuvitz (Ref. 16) were successfully used to design a circular iris matching discontinuity. This matching device maintains circular symmetry, which not only helps mode control, but also allows complete polarization flexibility.

IV. APPLICATIONS

Since the TM_{11}° mode does not radiate axially, the dual-mode conical horn has less axial gain than a dominant-mode conical horn with the same aperture size. Its use, therefore, is not dictated in applications requiring maximum aperture efficiency; most horn applications, however, are more concerned with pattern circularity and sidelobe performance. Obvious applications are for gain standards, anechoic chamber illuminators, and pattern range illuminators. One of the most important applications for the dual-mode conical horn is Cassegrainian feed systems. In such a system both the antenna aperture efficiency and the forward sidelobe level are critically dependent on the feedhorn beam efficiency characteristics (Ref. 17). The dual-mode horn was, in fact, developed for this application.

For some uses, the horn is an inconvenient structure because of its physical length in the direction of propagation. The popular horn reflector antenna (Ref. 18) was developed as an excellent solution to this problem. More recently a conical-horn reflector antenna has been developed (Ref. 19).

Although not yet experimentally investigated, it appears feasible to build a dual-mode conical-horn reflector antenna. Such an antenna would have the desirable sidelobe properties of the dual-mode conical horn combined with the physically convenient horn reflector configuration.

V. SUMMARY

A new type of conical-horn antenna has been described in which both the dominant TE_{11}° mode and the TM_{11}° mode are utilized to effect beamwidth equalization, phase center coincidence, and almost complete sidelobe suppression. The unusual performance of this type of horn is readily predicted by simple analysis. Complete experimental data is presented, showing the desired performance. Typical applications for pattern range illuminators, gain standards, and feedrorns are discussed.

REFERENCES

1. Silver, S., *Microwave Antenna Theory and Design,* McGraw-Hill Book Company, Inc., New York, 1949, Chapter 10.
2. Schelkunoff, S. A., and H. T. Friis, *Antennas Theory and Practice,* John Wiley and Sons, Inc., London, 1952, Chapter 16.
3. *Jasik, H., ed., Antenna Engineering Handbook,* McGraw-Hill Book Company, Inc., New York, 1961, Chapter 10.
4. Kraus, J. D., *Antennas,* McGraw-Hill Book Company, Inc., New York, 1950, Chapter 13.
5. Love, A. W., "The Diagonal Horn Antenna," *The Microwave Journal,* Vol. V, No. 3, March 1962, pp. 117-122.
6. Brueckman, H., "Suppression of Undesired Radiation from Directional HF Antennas and Associated Feed Lines," *Proceedings of the IRE,* Vol. 46, August 1958, pp. 1510-1516.
7. Southworth, G. C., *Principles and Applications of Waveguide Transmission,* D. Van Nostrand Company, Inc., Princeton, 1950, pp. 415-419.
8. Schorr, M. G., and F. J. Beck, "Electromagnetic Field of the Conical Horn," *Journal of Applied Physics,* Vol. 21, August 1950, pp. 795-801.
9. King, A. P., "The Radiation Characteristics of Conical Horn Antennas," *Proceedings of the IRE,* Vol. 38, March 1950, pp. 249-251.
10. Horton, C. W., "On the Theory of the Radiation Patterns of Electromagnetic Horns of Moderate Flare Angles," *Proceedings of the IRE,* Vol. 37, 1949, pp. 744-749.
11. Potter, P. D., *Suppressed Sidelobe Horn Antenna,* Invention Report No. 30-133, Jet Propulsion Laboratory, Pasadena, California.
12. Chu, L. J., "Calculation of the Radiation Properties of Hollow Pipes and Horns," *Journal of Applied Physics,* Vol. 11, 1940, pp. 603-610.
13. Jahnke, E., and F. Emde, *Tables of Functions,* Dover Publications, New York, 1945, Fourth Edition.
14. Potter, P. D., *The Aperture Efficiency of Large Paraboloidal Antennas as a Function of their Feed System Radiation Characteristics,* Technical Report No. 32-149, Jet Propulsion Laboratory, Pasadena, California, October 1961.
15. Cumming, R. C., "The Serrodyne Frequency Translator," *Proceedings of the IRE,* Vol. 45, February 1957, pp. 175-186.
16. Marcuvitz, N., *Waveguide Handbook,* MIT Radiation Laboratory Series, Vol. 10, McGraw-Hill Book Company, Inc., New York, 1951, Chapter 5.
17. Potter, P. D., "The Application of the Cassegrainian Principle to Ground Antennas for Space Communications," *IRE Transactions on Space Electronics and Telemetry,* Vol. 8, No. 2, June 1962.
18. Pippard, A. B., "The Hoghorn — An Electromagnetic Horn Radiator of Medium-Sized Aperture," *Journal of the IEE,* Pt. IIIA, Vol. 93, No. 10, 1946, pp. 1536-1538.
19. Leonard, M. V., "Bell Unveils Project Telstar Horn Antenna in Andover, Maine," *Microwave Journal,* Vol. V, No. 5, May 1962.